Technology and Health Care 16 (2008) 47–60
IOS Press

Tissue-level failure accumulation in vertebral cancellous bone: A theoretical model

Noa Slomka, Idit Diamant and Amit Gefen*
Department of Biomedical Engineering, Faculty of Engineering, Tel Aviv University, Tel Aviv, Israel

Received 14 August 2007
Revised 19 September 2007

Abstract. Vertebral compression fractures are a potentially severe injury, which is characteristic to osteoporotic elderly. Despite being a significant healthcare problem, the etiology of compression fractures is not fully understood, and there are no biomechanical models in the literature that describe the development of these fractures based on cancellous bone failure accumulation. The objective of this study was therefore to develop a computational model of tissue-level failure accumulation in vertebral cancellous bone, which eventually leads to compression fractures. The model predicts the accumulated percentage of broken trabeculae δ in a vertebral region of interest (ROI) over 60 years, by employing Euler's theory for elastic buckling. The accumulated failure δ is calculated as function of the daily activity characteristics and rate of annual bone loss (RABL) with aging. An RABL of unity represents the normal bone loss attributed to aging per se, whereas RABL$>$1 is assumed to represent pathological bone metabolism such as osteoporosis. Simulations were conducted for a range of RABLs, to determine the effect of changes in bone metabolism on the accumulation of bone failure. Results showed that bone failure rapidly increased with RABL. Generally, trabecular failure was shown to become more severe for RABL$>$4. Total failure was exhibited at RABL $=$ 7.5 for the central ROI, and at RABL $=$ 8.5 for the sub-endplate ROI. We concluded that vertebral compression fractures advance monotonically between the age of 50–55 years and 70 years, and may accelerate thereafter if RABL is high ($\sim$8). Additionally, the model identified weight lifting as the action that most dramatically accelerated the destruction of osteoporotic spinal cancellous bone. The present biomechanical model is useful for understanding the etiology of compression fractures, and potentially, depending on further experimental characterization of RABL, for considering the effects of medications that influence bone metabolism on patient prognosis.

Keywords: Osteoporosis, compression fractures, trabecular bone, buckling, model

1. Introduction

Vertebral compression fractures are a common injury among osteoporotic elderly [5,17,19]. Compression fractures can occur anywhere in the spine, from the occiput to the sacrum, but the most susceptible location is the thoracolumbar junction [27]. Symptoms are pain, and loss of height in case of multiple fracture locations. Complications include digestive and respiratory diseases and psychological implications such as depression and anxiety [5,26]. The main risk factor for vertebral compression fractures is low bone mineral density (BMD). For example, a person whose BMD is one standard deviation below his/her age-group norm has a 1.9-fold increased risk for a vertebral compression fracture [19]. Other risk factors include celiac disease [1], calcium malabsorption and cancer [6].

*Address for correspondence: Dr. Amit Gefen, Department of Biomedical Engineering, Faculty of Engineering, Tel Aviv University, Tel Aviv 69978, Israel. Tel.: +972 3 640 8093; Fax: +972 3 640 5845; E-mail: gefen@eng.tau.ac.il.

The vertebral body is mostly made up of cancellous bone. The cancellous bone is arranged in a three-dimensional (3D) lattice, comprised of vertical and horizontal trabeculae. As osteoporosis advances with old age, there is progressive reduction of BMD, trabecular thickness (Tb.Th) and trabecular connectivity accompanied by an increase of the trabecular separation (Tb.Sp) and trabecular length (Tb.L) [5,29]. As a result, the structural strength and stiffness of the cancellous bone diminish, which leads to greater vulnerability of the vertebral body to fractures under traumatic and non-traumatic mechanical loads. Importantly, osteoporotic-related vertebral compression fractures differ from other age-related fractures in that they may occur under loads applied during everyday ordinary activities such as lifting a light weight [5,36].

Evidence exists that the occurrence of compression fractures is associated with bending and buckling of trabeculae [8,14,23,29]. Specifically, Snyder et al. [29] examined the role of trabecular morphology changes in the etiology of compression fractures. They concluded that the most probable mode of deformation and mechanical failure of a spinal trabecula is buckling. The vertical trabeculae serve as structural columns that support compressive loads (either body-weight alone or body-weight and external loads). The horizontal trabeculae act as cross-struts stabilizing the columns. As the Tb.Sp of the horizontal trabeculae increases, the effective length of the vertical trabeculae also increases, and this decreases their mechanical stability under compressive loads. Eventually, vertical trabeculae buckle and break, which causes deformity of the affected vertebras, and correspondingly, gross distortion of the spine [29].

Since vertebral compression fractures are a significant healthcare problem, which is likely to increase as the population ages, there is a need to better understand cancellous bone failure mechanisms that lead to fracture development. Nevertheless, a biomechanical model able to simulate the onset and progression of compression fractures is missing in the literature. The only two relevant publications in this regard are by Keller et al. [18] and Ramtani and Abdi [28]. Keller et al. [18] analyzed the influence of compression fractures on the gross shape of the spine, however, they did not consider the mechanism of fracture at the bone tissue level, i.e., at the scale of individual trabeculae. Ramtani and Abdi [28] utilized Cowin's concepts of adaptive elasticity [10,16] to formulate a trabecular bone-plate buckling theory that exhibits the possible influence of bone remodeling on bone-plate buckling. Nevertheless, they did not consider failure accumulation in response to different loads applied to the bone. That is, they did not simulate fracture development with time. Accordingly, the objective of the present study was to develop a model able to simulate the onset and progression of tissue-level trabecular failure in vertebrae of elderly over time, under daily loading. The model inputs include the initial spinal trabecular morphology at the time of skeletal maturity, the daily loading characteristics and the rate of bone loss with aging. The model outputs are predictions of the extent of tissue-level failure, namely, the percentage of failed trabeculae, as function of age. Thus, the model provides information that is important for understanding the prognosis of compression fractures, and is particularly useful for approximating the potential effectiveness of pharmaceutical treatments affecting the rate of bone loss.

2. Methods

A computational model able to simulate the development of compression fractures over time in a vertebral region of interest (ROI), as function of the loading scenario and rate of cancellous bone loss, was developed. The model was implemented in a software code that calculates percentage of broken trabeculae in the ROI after each cycle of repeatedly applied loading scenario simulating daily activities. The model considers the decrease in Tb.Th and increase in Tb.L that are characteristic to the elderly, and

so, Tb.Th and Tb.L are updated for all intact trabeculae at each simulation time-step (that is, 1 year). The specific inputs to the model are the number of trabeculae in a single vertebral layer comprising an ROI, the weekly loading scenario, the modulus of elasticity of cancellous bone at the tissue-level, initial distributions of Tb.Th dimensions and initial Tb.L, the number of simulated years, initial age, body weight and the rate of annual bone loss (RABL) affecting the time-dependent Tb.Th and Tb.L.

2.1. Measurements of trabecular dimensions

Trabecular dimensions used for model calculations (Tb.Th, Tb.L) were based on in vitro measurements. Cancellous bone samples were extracted from lumbar vertebrae (L1 and L5) of 3 human cadavers without any known musculoskeletal disease, in order to measure Tb.Th and Tb.L under digital optical microscopy (magnification $\times$30, Axiolab A, Zeiss Co.). From each vertebra, a flat (2–3 mm thick) cancellous bone sample was extracted. Specimens were first cleaned by means of vacuum to remove marrow. Dimensions of about 30 trabeculae per specimen were measured using the method described in Dagan et al. [11]. The range of Tb.Th obtained through these measurements was 0.27-fold to 1.9-fold the average Tb.Th, which was 170 ± 45 μm (mean $\pm$ standard deviation). The range of Tb.L obtained was 0.4-fold to 2-fold the average Tb.L, which was 420 ± 150 μm. The distributions of measured Tb.Th and Tb.L values are shown in Figs 1a and 1b, respectively.

2.2. Computational model

The ROI in vertebral cancellous bone was selected to be a single layer of trabeculae over a full vertebral cross-sectional area in the lumbar spine. The second lumbar vertebra (L2) was selected for all simulations. An illustration of the different trabecular shapes in an ROI is provided in Fig. 2. Two ROIs in vertebra L2, that is, the sub-endplate and central vertebral ROIs were investigated separately. These two regions differ in their cancellous bone microarchitecture [32]. Specifically, for the sub-endplate ROI, Tb.Th was assigned distribution according to our morphological measurements (with mean of 170 μm, Fig. 1a), however, according to Thomsen et al. [32], mean Tb.Th at the age of 30 is $\sim$10 μm larger for the central region than for the sub-endplate region. Therefore, mean Tb.Th for the central ROI was taken as 180 μm and thickness distribution was adjusted correspondingly, while maintaining the same pattern of distribution revealed in our measurements (Fig. 1a). The Tb.L was set as the mean of our measurements, i.e. 420 μm, for both regions (Fig. 1b), and all trabeculae in the ROIs were assigned the same initial length. The number of trabeculae in each ROI was calculated as the number of trabeculae found in a square mm multiplied by the cross-sectional area of the region. Cross-sectional area was taken as 1280 mm^2 for the sub-endplate ROI [31] and as 1126 mm^2 for the central ROI [22]. The number of trabeculae in a square mm was adopted from Thomsen et al. [32] as 1.5 mm^{-2} for the sub-endplate ROI and as 0.8 mm^{-2} for the central ROI, assuming that vertebral cancellous bone is arranged as a perfect 3D lattice.

The present model employs the single-trabecula generic ‘building block’, which was described in detail in Dagan et al. [11] and was employed by our group in several previous studies [3,4,11–13]. In brief, the trabecula ‘building block’ is an idealization of the geometry of an individual trabecula, which is based on statistical analyses of the dimensions of 200 trabeculae. The profile shape of the ‘building block’ is:

$$r(z) = \pm\frac{2Tb.Th - \beta}{1+\alpha}\left\{\mathrm{COS}\left(\frac{2Z}{L}\mathrm{COS}^{-1}\left(\frac{1}{2}\left(3-\alpha-\frac{\beta(1+\alpha}{2Tb.Th-\beta}\right)\right)\right)-\frac{3}{2}\right\} \quad (1)$$

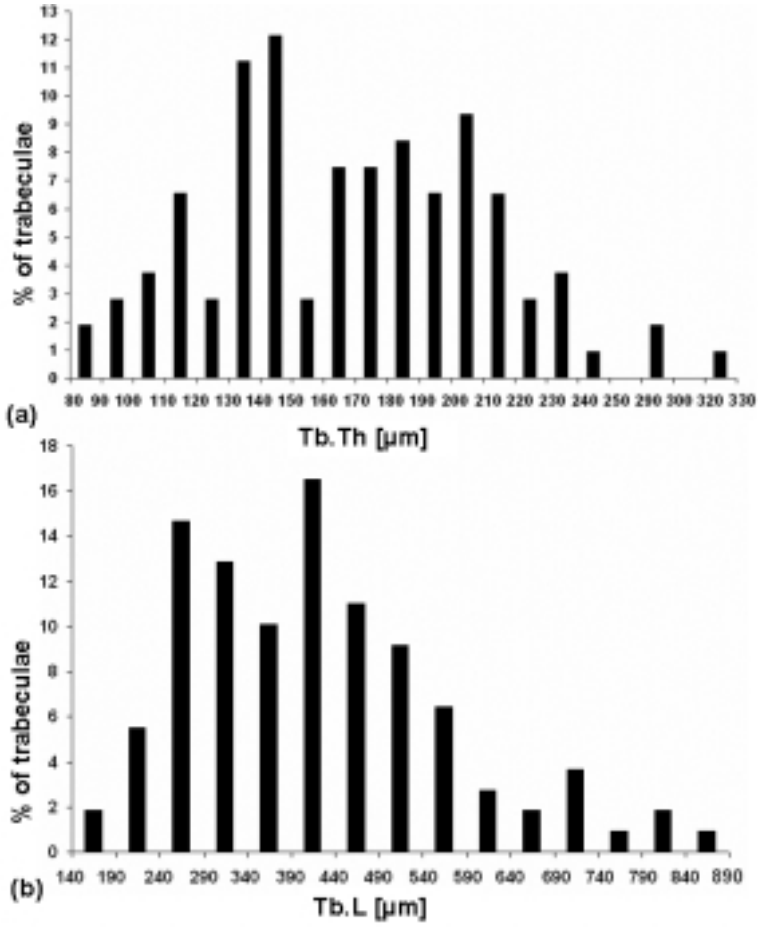

Fig. 1. Cancellous bone microarchitecture: (a) Histogram of measured trabecular thickness (Tb.Th) dimensions of 100 human trabeculae from the lumbar spine. (b) Histogram of measured corresponding trabecular length (Tb.L) dimensions.

where $r(z)$ is the radius of the generic trabecula at location z along its length ($z = 0$ is the center of the trabecula), Tb.Th is the mean thickness of the trabecula across its length (L) and the empirical constants are $\alpha = 1.3736$ and $\beta = 40.9$ μm [11].

Each time a mechanical load is applied to an ROI, it is distributed across all intact trabeculae in that ROI, and each individual trabecula supports a fraction of the total load that is proportional to its relative axial stiffness. Thus, the force acting on each individual trabecula $P_i^{(t)}$ at a discrete time t when the ROI is subjected to a total load $P_L^{(t)}$ is:

$$P_i^{(t)} = \frac{EA_i}{\sum_{j=1}^{N} EA_j} P_L^{(t)} \tag{2}$$

where E is the elastic modulus of cancellous bone at the tissue-level, A_i is the mean cross-sectional area of an individual trabecula i, and N is the number of intact trabeculae in the ROI. The tissue-level modulus of elasticity E was set as 11 GPa for all trabeculae [11]. The cross-sectional area of trabeculae

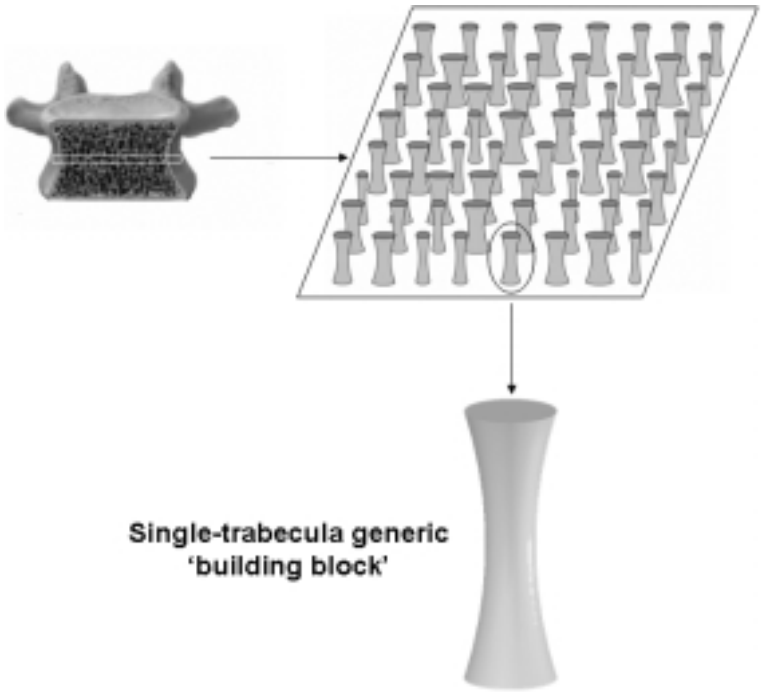

Fig. 2. Illustration of different shapes of trabeculae in a region of interest (ROI) in spinal cancellous bone, based on the representation of the single trabecula generic 'building-block' [10].

A_i at their center ($z = 0$) is calculated from Eq. (1) as:

$$A_i = \frac{\pi}{4} \cdot \left(\frac{2 \cdot Tb.Th - \beta}{1 + \alpha} \right)^2 \tag{3}$$

The load applied to each trabecula $P_i^{(t)}$ is compared to its critical load for buckling P_i^{cr}, which is calculated according to Euler's theory for elastic buckling:

$$P_i^{cr} = \frac{\pi^2}{k^2} E A_i \left(\frac{2 \cdot Tb.L_i}{Tb.Th_i} \right)^{-2} \tag{4}$$

where k is a boundary condition constant taken as 0.5 assuming that trabeculae may resist bending moments at both ends [7]. Each P_i^{cr} value is calculated at the center of the trabecula ($z = 0$) where thickness is minimal Eq. (1), since at this location, peak compression stresses occur. A trabecula is considered to buckle and fail if the applied load at any time $t, P_i^{(t)}$, is greater than, or equal to its critical load for buckling P_i^{cr} Eq. (4).

Changes in bone metabolism with aging, as manifested in the trabecular microarchitecture, were integrated into model calculations. Specifically, an annual Tb.Th decrease was considered based on measurements by Thomsen et al. (2002) [33], as 0.114 μm/year and 0.138 μm/year for the sub-endplate and central ROIs, respectively. Annual elongation of trabeculae, manifested by an increase in Tb.L, was similarly considered, and was set as 2.2 μm/year for both regions [30]. These values, adopted from studies on the effect of normal aging on the trabecular microarchitecture, were assumed to reflect age-related changes in bone metabolism per se, that is, without considering accelerated bone loss owing

to osteoporosis. In order to simulate osteoporosis-related changes as well, we further increased the above loss rates, as described in the "protocol of simulations" section.

The model was implemented using Matlab7 (MathWorks Co., Natick, Ma, USA) and a flowchart of the software code is presented in Fig. 3. The software code calculates the failure accumulation in spinal cancellous bone iteratively. For each phase of a weekly loading scenario, the model compares between the actual loads applied to individual trabeculae and corresponding critical buckling loads. All trabeculae that experience loads greater than or equal to the critical load are marked as failed, and are considered as not being able to bear loads thereafter. The calculation is performed 52 times, for each week of a year. On each time step, the compressive load applied to ROIs is distributed only between trabeculae that did not fail previously. Hence, the load applied to the still intact trabeculae increases if some trabeculae failed at previous simulation steps. After completing a full year, the thickness and length of trabeculae are updated, and the process is repeated again for 60 years. Simulations are terminated if all trabeculae in the ROI have failed.

2.3. Protocol of simulations

The initial age was set as 30 years in all simulations. Likewise, all simulations were terminated at the age of 90 years. Bodyweight was set as 80 kg. The weekly loading scenario consisted of 5,000 gait cycles per each day of the week [22] followed by lifting 5 kg two times per week, to represent weekly routine tasks such as grocery shopping or some housework. The force applied to the ROIs in the L2 vertebra during each gait cycle was set to be 1.6 times the body weight, which is the peak lumbar vertebral load occurring during normal gait [20]. The force applied to the ROIs during the lifting tasks was calculated from the equilibrium of force equations provided by Lindh [20], which yielded a vertebral load of 3400 N per each lifting maneuver.

In order to determine the effect of changes in bone metabolism on the accumulation of bone failure, simulations were conducted for a range of rates of annual bone loss (RABL). An RABL of unity represents the normal bone loss which is attributed to aging per se, whereas RABL>1 is assumed to represent pathological bone metabolism such as osteoporosis. For each simulation, the decrease in Tb.Th and the increase in Tb.L at the completion of a full year are:

$$Tb.Th(\text{year}) = Tb.Th^{30y} - RABL \cdot \eta \cdot (\text{year} - 1) \tag{5}$$

$$Tb.L(\text{year}) = Tb.L^{30y} + RABL \cdot \mu \cdot (\text{year} - 1) \tag{6}$$

where $Tb.Th^{30y}$ and $Tb.L^{30y}$ are the Tb.Th and Tb.L at the age of 30 years, respectively, and η and μ are the annual decrease in Tb.Th and annual increase in Tb.L owing to normal aging ($\eta = 0.114$ μm/year for the sub-endplate ROI; $\eta = 0.138$ μm/year for the central ROI; $\mu = 2.2$ μm/year for both ROIs [29, 32]. The effect of RABL on accumulation of bone failure was studied by determining the percentage of failed trabeculae (δ) at each ROI for increasing RABL values, at steps of 0.5 (Eqs 5,6). Simulations were aborted when all trabeculae (100%) failed. For the sub-endplate ROI, this occurred when RABL $=$ 8.5; for the central ROI, total failure occurred when RABL $= 7.5$.

2.4. Model sensitivity to parameters

In order to determine the sensitivity of model predictions of percentage of failed trabeculae (δ) to the values of model input parameters, we ran sensitivity analyses, changing one parameter value at a time,

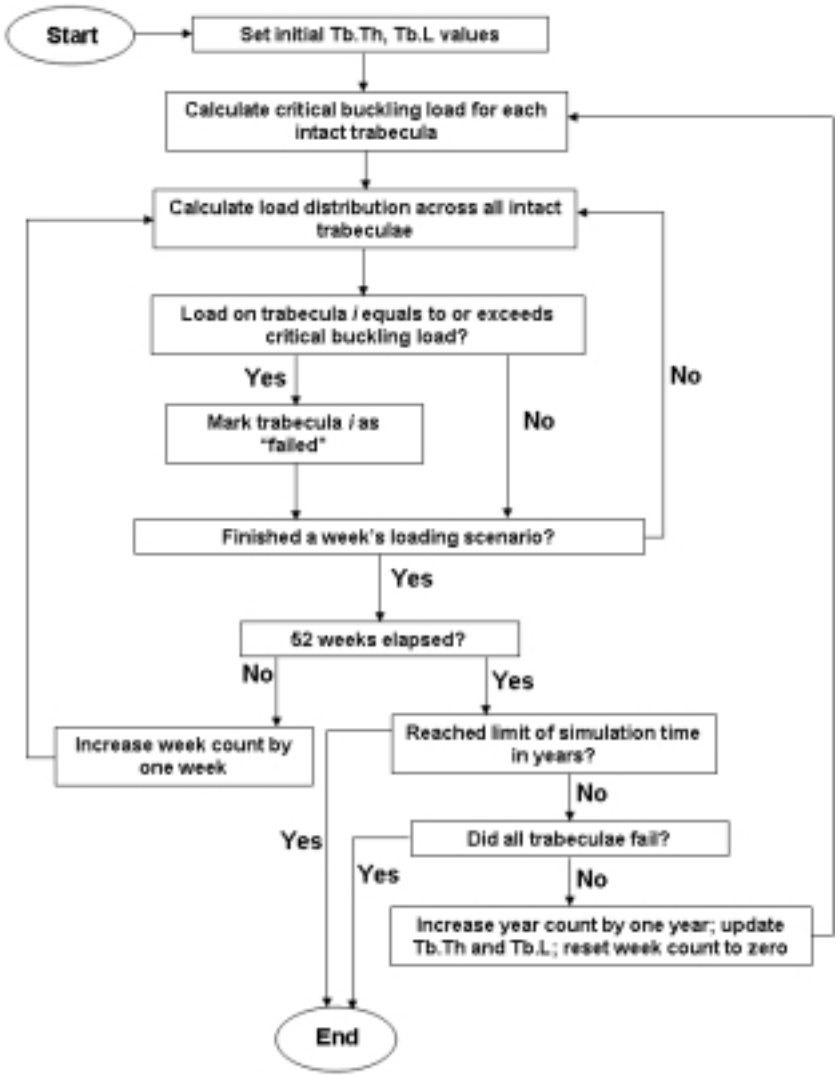

Fig. 3. A flowchart of the software code (Tb.Th = trabecular thickness, Tb.L = trabecular length).

while keeping all other parameters at their nominal values (which were provided above). Specifically, we tested the variation in model predictions in response to ± 20 kg change in body weight, $+8$ kg and -4 kg change in weights lifted every week, a case where no weights are lifted at all, change of $\pm 20\%$ in the number of trabeculae per ROI, and a 17% reduction of the tissue-level modulus of elasticity of cancellous bone to 9.1 GPa [9]. Sensitivity analyses were conducted for RABL = 3 and RABL = 6.

3. Results

3.1. Computational simulations

The percentages of failed trabeculae (0–100%) in the central and sub-endplate ROIs between the ages of 30 and 90 years, as a function of the RABL, are shown in Fig. 4. Overall, the percentage of failed

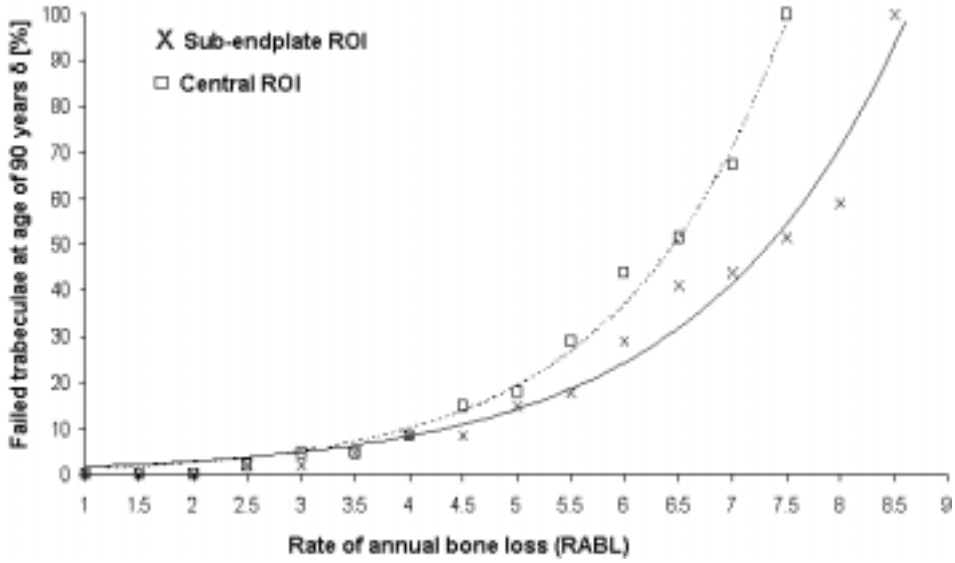

Fig. 4. Percentage of failed trabeculae δ between the ages of 30 and 90 years as a function of the rate of annual bone loss (RABL). Marks indicate direct computation of model results, and lines indicate fits of exponential curves to the discrete model data.

trabeculae δ increased with RABL, according to the exponential relation:

$$\delta = \sigma \cdot \exp\left(\upsilon \cdot RABL\right) \tag{7}$$

where σ and υ are constants derived from curve fitting. For the sub-endplate ROI these constants were $\sigma = 0.97$ and $\upsilon = 0.54$ (correlation coefficient $R^2 = 0.96$). Similarly, the constants for the central ROI were $\sigma = 0.74$ and $\upsilon = 0.65$ ($R^2 = 0.99$). For RABL $= 1$, which represents bone loss due to normal aging, no significant vertebral damage was predicted by the model. As RABL increased, with the level of severity of osteoporotic bone loss, bone failure rapidly increased as well (Fig. 4) whereas failure of trabeculae occurred slightly faster in the central ROI. Assuming that a 10% of failed spinal trabeculae is a reasonable level of damage that can be compromised at old age, the model indicates that RABL should be kept below 4 (Fig. 4). Total failure was exhibited at RABL $= 7.5$ for the central ROI, and at RABL $= 8.5$ for the sub-endplate ROI. The accumulated failure of trabeculae as a function of age in the sub-endplate ROI is depicted in Fig. 5 for RABL $= 5.5$ and RABL $= 8$. For RABL $= 5.5$, failure of trabeculae first appeared at the age of 57 years. However, for RABL $= 8$, failure of trabeculae started much earlier, at the age of 49 years. Likewise, accumulated trabecular failure δ for RABL $= 5.5$ was substantially lower at the simulated age of 90 years ($\sim$18%), compared with the RABL $= 8$ case ($\sim$59%). Taking the above results together, we conclude that vertebral compression fractures owing to osteoporosis onset at an age of around 50–55 years, progress monotonically until an age of around 70 years, and may accelerate considerably at older ages if RABL is high ($\sim$8, Fig. 5). Overall, trabecular failure becomes more severe for RABL$>$4, where there is a "toe region" of the δ-RABL curve (Fig. 4), and so, the present model indicates that the aim of minimizing the occurrence of osteoporotic compression fractures should be to reduce RABL at least below 4.

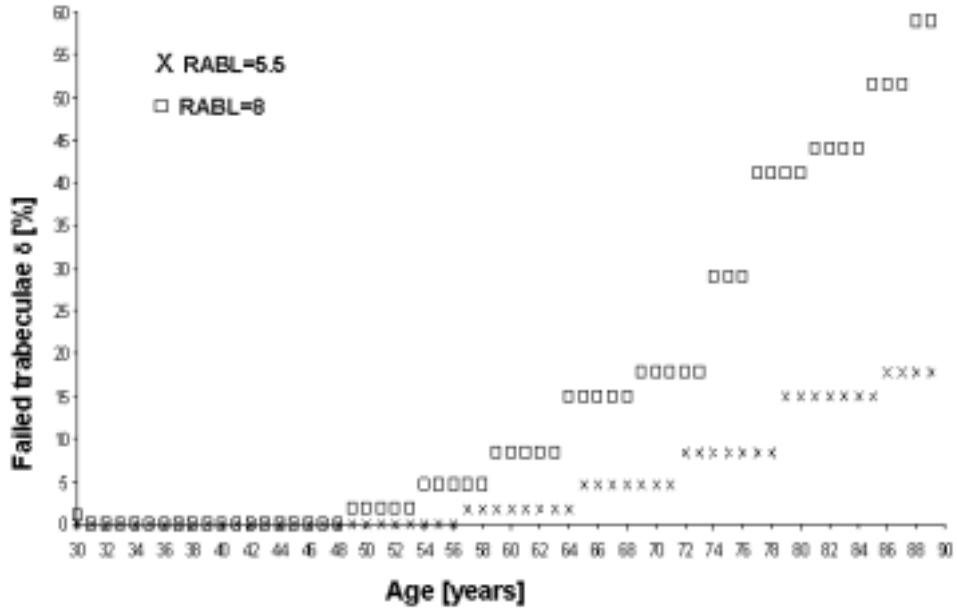

Fig. 5. Percentage of failed trabeculae δ as a function of age in the sub-endplate region of interest (ROI). RABL = rate of annual bone loss.

3.2. Model sensitivity to parameters

Sensitivity analyses revealed that changes in values of all model parameters had greater effect on δ for RABL $= 6$ than for RABL $= 3$ (Table 1). Generally, the sub-endplate and central ROIs were affected by the parameter variation to a similar extent, for both RABL $= 3$ and RABL $= 6$. Specifically, for RABL $=$ 3, changes in predictions were in the range of -2% to $+3\%$ for the variations in model parameters that were specified in the methods section. For RABL $= 6$, corresponding changes in predictions were in the range of -21% to $+12\%$. The model was found to be insensitive to changes in parameter values for RABL $= 1$. Weight lifting activity had the greatest effect on model predictions (Table 1). Specifically, when no weight at all was lifted, and for RABL $= 3$, decreases of 2% and 5% in δ were demonstrated for the sub-endplate and central ROIs, respectively. For the same simulation case, but with RABL $= 6$, decreases of 21% and 29% in δ were demonstrated in the sub-endplate and central ROIs, respectively. We found no change in δ for any increase above 2 in the number of times per week that a given weight is lifted. The model was also insensitive to the number of steps per day. The analyses further showed that model sensitivity to moderate changes in bodyweight, external weights lifted, the number of trabeculae in the ROI, and the tissue-level elastic modulus of cancellous bone was similar (Table 1). Taking these results together, we conclude that avoiding weight lifting at old age is the most influencing action predicted by the model to minimize the risk for compression fractures.

4. Discussion

This study was focused on the biomechanics of formation and development of human vertebral compression fractures, which are mainly attributed to osteoporosis. The mechanism ascribed to as responsible for these fractures is buckling of a large number of trabeculae. A computational model

Table 1
Sensitivity analyses: effects of variation in model parameters on failure accumulation predictions δ in the sub-endplate and central regions of interest (ROIs). The change in failure accumulation predictions is calculated as the difference between δ with altered model parameters and δ with nominal parameter values

Model input parameters		Effects on model predictions			
Parameter type	Variation	Change in failure accumulation prediction			
		Sub-endplate ROI		Central ROI	
		RABL = 3	RABL = 6	RABL = 3	RABL = 6
Body weight	+20 kg	3%	12%	0%	7%
	−20 kg	0%	−11%	−3%	−15%
Weight lifted every week	+8 kg	3%	12%	0%	7%
	−4 kg	0%	−11%	−3%	−3%
Number of times per week a weight is lifted	−2	−2%	−21%	−5%	−29%
Number of trabeculae in ROI	+20%	0%	−11%	−3%	−15%
	−20%	3%	12%	0%	7%
Tissue-level modulus of elasticity	−17%	3%	12%	0%	7%

able to simulate the progression of compression fractures with age as a function of the combination of the loading protocol (constituted by daily activity) and metabolic bone changes over time in a single layer of trabeculae was developed. Simulations were conducted to determine the failure accumulation in trabeculae of the lumbar spine from skeletal maturity at 30 years old, up to the age of 90 years, for different intensities of activity and bone loss rates.

The model indicated that vertebral compression fractures start to develop at ages of 50–55 years, and that the intra-vertebral damage progresses at a nearly constant rate until the age of about 70 years, after which failure accumulation in the spinal cancellous bone accelerates substantially if the RABL is high (i.e. $\sim$8). The model also identified weight lifting as being the action that most dramatically accelerated the destruction of the spinal cancellous bone. In contrast, increased walking activity did not contribute to the failure accumulation at all.

Model results showed that for RABL $= 1$ nearly no failure occurred over the time period of 60 years for both ROIs. This is well expected, since vertebral compression fractures are clinically related to osteoporosis (i.e. RABL$>$1), but not to normal aging. As RABL was increased in our simulations, accumulated failure δ increased correspondingly in an exponential pattern for both ROIs, although this increase was somewhat faster for the central ROI. This result gives a good second indication of the model's reliability since most vertebral fractures are clinically described as wedge or burst fractures that originate at the core of the vertebral body [25].

The model predicts that ideally, RABL should be kept within the range of 1–2 over adulthood, and in worse cases of bone loss rates, RABL should be kept at least below 4. The strength of the present model is in its ability to predict the effects of any treatment (medication, physical exercise, vitamins) which potentially influence RABL (assuming that the altered RABL can be quantified), on the prognosis of spinal cancellous bone damage. Yet, as direct experimental validation of the present model is extremely difficult to achieve, results should be interpreted as trends of effects, not as absolute numbers. With that being said, it is still useful to compare the RABL values used herein with respect to available clinical data. Specifically, in this study, we defined the rate of annual bone loss (RABL) depending on the trabecular thickness (Tb.Th) and trabecular length (Tb.L). The Tb.Th was found to decrease linearly with the decrease in bone density, whereas the Tb.L increases linearly with the decrease in density [29]. Hence, this empirical linearity allows some comparisons of RABL values predicted by the present model as leading to vertebral fragility at old age, with experimentally-found bone loss rates in fracture and non-fracture subject groups. Epidemiological studies in a cohort of 614 healthy women

aged 24–44 years revealed that the rate of change in bone density varies within a range of up to 3.5-times the mean rate of density change [2]. This is in good agreement with the present finding that RABL up to 4 is tolerable and leads to minimal bone damage at old age, that is, RABL between 1–4 can be associated with "normal aging". In another cohort, of 966 women, the rate of bone density change was found to be 2.6-fold higher in the sub-group who suffered osteoporotic vertebral fractures at old age, compared with those who did not [24]. Extrapolating this to the present computational predictions, by multiplying the predicted midrange of RABL for "normal aging" (2.5) by the ratio of fracture over non-fracture bone loss rates (2.6) from the Nguyen study [24] indicates that an RABL of $2.5 \times 2.6 = 6.5$ is of high risk for a vertebral compression fracture. Again, this is in good agreement with our simulations, which predict total failure of vertebrae for RABL above 7.5. Taken together, the above literature [2,24,29] therefore indicates that the range of RABL values that were used in the present simulations (Figs 4,5) are physiologically reasonable.

The model described herein is based on several assumptions and therefore has some related inevitable limitations which should be considered when interpreting the results. The first limitation concerns the horizontal trabeculae in the vertebra: While it may appear as if the horizontal trabeculae were not accounted for in the modeling, their structural contribution was indirectly taken into account by introducing elongation of vertical trabeculae with time, which represents the progressive resorption and failure of the horizontal trabeculae.

Second, in order to employ the Eulerian buckling theory Eq. (4), it was assumed that when unloaded, trabeculae are oriented parallel to the load axis and that their failure always occur by elastic buckling in the first mode [7]. It should be noted, however, that if the trabecular orientation is not parallel to the direction of the external load then buckling may occur under lower load magnitudes (though individual buckling events will be more difficult to predict). Hence, the model may be somewhat overoptimistic in regard to the predicted strength of the cancellous bone structure with respect to real-world conditions.

A third limitation is that the model was developed for studying ROIs in a vertebra, not a whole vertebra. However, the ROI approach still provides good indications of the trabecular failure behavior, and the gross differences in proximity or far from the end-plates. In future development of the present modeling concept, the work can be expanded to represent a complete vertebra by introducing many (not just two) structural layers of trabeculae, and by further considering the layer-to-layer biomechanical interactions.

Fourth, it was assumed that each time a load is applied to an ROI, that load is distributed across all intact trabeculae. In the design of the model, it was possible to assume either a "force control", that is, that an external force on the vertebra is distributed across all the trabeculae, or to assume a "displacement control", that is, that trabeculae are all displaced together to a given extent when loaded. These two "control" modes are actually equivalent if it is imposed that the thinner, more compliant trabeculae will experience less force than the thicker ones. In the present model, this is obtained by distributing the external load across trabeculae proportionally to their relative axial stiffnesses (Eq. 2). The concept that compression loads are distributed across trabeculae proportionally to their axial stiffnesses is based on finite element analyses by Homminga and colleagues [15]. Specifically, their work indicated that physiological loads on vertebrae are distributed over the whole trabecular core, and at the central core region, loads are more intense than at the peripheries (see Fig. 3b in their paper). Taken together with the histomorphometric data of Thomsen [32] that indicates a thicker cross-section for central trabeculae, it appears that indeed, load sharing correlates with the distribution of axial stiffnesses of trabeculae.

Fifth, we did not include microcrack repair (remodeling) and microfracture repair in our computer simulations in lack of experimental data on the effect of age on the repair rate of trabeculae in humans. Though very recently, it was published that the repair of microdamage in trabeculae slows down with

age [37], the experimental data are available only for rats, and in the rats, only for two specific age groups, and just for the femur [37]. More experimental data are therefore required, desirably from humans, and specifically for vertebrae, in order to add the feature of repair of trabeculae to our model. We expect that such addition to the model will reduce the overall rate of failure accumulation, but as the rate of repair is likely to decrease substantially at old ages [37], where damage accumulates rapidly (Fig. 5), it is difficult to predict whether the addition of the repair feature to the model will have a significant influence.

Last, other than ignoring remodeling at this stage, we also did not consider trabecular bone modeling and adaptation to altered mechanical use [3]. Some elderly may suffer additional bone loss to that described by Eqs (5,6) owing to inactive or sedentary lifestyle, limited mobility and bed confinement, or chronic muscular weakness (age-related sarcopenia) [3]. Likewise, some medications commonly consumed at old age, such as statins, may affect the RABL. Finally, diseases that are more prevalent at old age, including diabetes type II and hyperlipidemia, were associated epidemiologically with osteoporosis, and may also affect the RABL [34]. Detailed, experimental quantitative characterization of the effect of each of these conditions on the RABL will be required before practical implementation of the model proposed herein can be realized.

The model herein takes into consideration various input conditions, including trabecular microarchitectural characteristics, tissue mechanical properties, and the formulation of metabolic bone changes. Many simulation scenarios, originating from different input parameter combinations can be applied to the model, e.g. other spine locations, an osteoporotic stage at young age, changes in body weight throughout life or some unusual activity profiles. Hence, the model can be considered as a generic biomechanical tool that can be implemented in numerous desired applications. For this reason, the present model shows the raw potential to perform as patient-specific in the future.

In closure, the feasibility of a model describing tissue-level failure accumulation in vertebral cancellous bone, as related to onset and progression of spinal compression fractures, was demonstrated in this paper. The present model shows a great potential to serve as a predictive biomechanical and clinical tool for the prognosis of vertebral fracture development under individual circumstances. Successful implementation however, depends on experimental studies to determine the age-dependent repair rate in human vertebral cancellous bone, as well as on the quantification of the altered RABL in conditions affecting the mechanical stimuli applied to the skeleton (such as disuse or sarcopenia) [3], chronic diseases that apparently affect bone metabolism (e.g. diabetes, hyperlipidemia) [34], and medications prescribed in these conditions, which further affect the bone metabolism (e.g. statins).

Acknowledgement

This study was supported (in part) by grant no. 5918 from the Chief Scientist's Office of the Ministry of Health, Israel (AG).

References

[1] O. Armagon, F. Tascioglu, O. Colak, C. Oner and Y. Akgum, Serological screening for celiac disease in premenopausal women with idiopathic osteoporosis, *J Rheumatol* **24** (2005), 239–243.
[2] K.E. Bainbridge, M.F. Sowers, M. Crutchfield, X. Lin, M. Jannausch and S.D. Harlow, Natural history of bone loss over 6 years among premenopausal and early postmenopausal women, *Am J Epidemiol* **156** (2002), 410–417.
[3] M. Be'ery-Lipperman and A. Gefen, Contribution of muscular weakness to osteoporosis: computational and animal models, *Clin Biomech* **20** (2005), 984–997.

[4] M. Be'ery-Lipperman and A. Gefen, A method of quantification of stress shielding in the proximal femur using hierarchical computational modeling, *Comput Methods Biomech Biomed Engin* **9** (2006), 35–44.
[5] M. Bono and A. Einhorn, Overview of osteoporosis: pathophysiology and determinants of bone strength, *Eur Spine J* **12** (2003), S90–S96.
[6] S. Brunton, B. Carmicheal, D. Gold, B. Hull, T. Kauffman, A. Papaioannou, R. Rasch, H. Stracke and E. Truuumees, Vertebral compression fractures in primary care, *J Fam Pract* **54** (2005), 781–788.
[7] D.O. Brush and B.O. Almroth, *Buckling of Bars, Plates and Shells*, McGraw-Hill, New York, 1975.
[8] D.R. Carter and W.C. Hayes, Bone compressive strength: the influence of density and strain rate, *Science* **194** (1976), 1174–1176.
[9] A.M. Coats, P. Zioupos and R.M. Aspden, Material properties of subchondral bone from patients with osteoporosis or osteoarthritis by microindentation testing and electron probe microanalysis, *Calcif Tissue Int* **73** (2003), 66–71.
[10] S.C. Cowin and D.M. Hegedus, Bone remodeling I: theory of adaptive elasticity, *J Elast* **6** (1976), 313–325.
[11] D. Dagan, M. Be'ery and A. Gefen, Single-trabecula building-block for large-scale finite element models of cancellous bone, *Med Biol Eng Comput* **42** (2004), 549–556.
[12] I. Diamant, R. Shahar and A. Gefen, How to select the elastic modulus for cancellous bone in patient-specific continuum models of the spine, *Med Biol Eng Comput* **43** (2005), 465–472.
[13] I. Diamant, R. Shahar, Y. Masharawi and A. Gefen, A method for patient-specific evaluation of vertebral cancellous bone strength: in vitro validation, *Clin Biomech* **22** (2007), 282–291.
[14] L.J. Gibson, The mechanical behavior of cancellous bone, *J Biomech* **18** (1985), 317–328.
[15] J. Homminga, H. Weinans, W. Gowin, D. Felsenberg and R. Huiskes, Osteoporosis changes the amount of vertebral trabecular bone at risk of fracture but not the vertebral load distribution, *Spine* **26** (2001), 1555–1561.
[16] D.M. Hegedus and S.C. Cowin, Bone remodeling II: small strain adaptive elasticity, *J Elast* **6** (1976), 337–352.
[17] M. Karlsson, C. Obrant and P.O. Jossefson, Osteoporotic fractures, in: *Rockwood and Green's Fractures in Adults*, R.W. Buchloz, J.D. Heckman, C. Court-Brown, P. Torentta, K.J. Koval and M.A. Wirth, eds, Lippincott Williams and Wilkins, Philadelphia, 2005, pp. 613–630.
[18] T.S. Keller, D.E. Harrison, C.J. Colloca, D.D. Harrison and T.J. Janik, Prediction of spinal deformity, *Spine* **28** (2003), 455–462.
[19] M. Lane, L. Russel and S. Khan, Osteoporosis, *Clin Orthop* **372** (2000), 139–150.
[20] M. Lindh, Biomechanics of the lumbar spine, in: *Basic Biomechanics of the Musculoskeletal System*, M. Nordin and V. Frankel, eds, Lea and Febiger, London, 1989, pp. 183–208.
[21] T.M. Link, M. Doren, G. Lewing, N. Meier, A. Heiniche and E. Rummery, Cross-sectional area of lumbar vertebra in peri- and postmenopausal patients with and without osteoporosis, *Osteoporos Int* **11** (2000), 304–309.
[22] K.S. Maluf and M.J. Mueller, Comparison of physical activity and cumulative plantar tissue stress among subjects with and without diabetes mellitus and a history of recurrent plantar ulcers, *Clin Biomech* **18** (2002), 567–575.
[23] R. Muller, S.C. Gerber and W.C. Hayes, Micro-compression: a novel method for the non destructive assessment of bone failure. *J Biomech* **31**(S1) (1998), 150.
[24] T.V. Nguyen, J.R. Center and J.A. Eisman, Femoral neck bone loss predicts fracture risk independent of baseline BMD, *J Bone Miner Res* **20** (2005), 1195–1201.
[25] J.I. Old and M. Calvert, Vertebral compression fractures in the elderly, *Am Fam Physician* **69** (2004), 111–116.
[26] A. Papaioannou, N.B. Watts, D.L. Kendler, C.K. Yuen, J.D. Adachi and N. Ferko, Diagnosis and management of vertebral fractures in elderly adults, *Am J Med* **113** (2002), 220–228.
[27] U. Patel, G.A. Campbell, A.J. Crisp and I.T. Boyle, Clinical profile of acute vertebral compression fractures in osteoporosis, *Br J Rheumatol* **30** (1991), 418–421.
[28] S. Ramtani and M. Abdi, Buckling of adaptive elastic bone-plate: theoretical and numerical investigation, *Biomech Model Mechanobiol* **3** (2005), 200–208.
[29] B.D. Snyder, S. Piazza, W.T. Edwards and W.C. Hayes, Role of trabecular morphology in the etiology of age-related vertebral Fractures, *Calcif Tissue Int* **53** (1993), S14–S22.
[30] P. Sutton-Smith, I.H. Parkinson, A.M.J. Linn, S.A. Kooke and N.L. Fazzalari, Trabecular rod buckling index in Thoraco-Lumbar vertebral bone, *Clin Anat* **19** (2006), 12–18.
[31] S.H. Tan, E.C. Teo and H.C. Chua, Quantitative three-dimensional anatomy of lumbar vertebrae in Singaporean Asians, *Eur Spine J* **11** (2002), 152–158.
[32] J.S. Thomsen, E.N. Ebbesen and L.I. Mosekilde, Zone-dependent changes in human vertebral trabecular bone: clinical implications, *Bone* **30** (2002), 664–669.
[33] J.S. Thomsen, E.N. Ebbesen and L.I. Mosekilde, Age-related differences between thinning of horizontal and vertical trabeculae in human lumbar bone as assessed by a new computerized method, *Bone* **31** (2002), 136–142.
[34] Y. Tintut, S. Morony and L.L. Demer, Hyperlipidemia promotes osteoclastic potential of bone marrow cells ex vivo, *Arterioscler Thromb Vasc Biol* **24** (2004), e6–10.
[35] P.R. Townsend, R.M. Rose and E.L. Radin, Buckling studies of single human trabeculae, *J Biomech* **8** (1975), 199–201.

[36] H.A. Yuan, C.W. Brown and F.M. Phillpis, Osteoporotic spinal deformity: A biomechanical rationale for the clinical consequences and treatment of vertebral body compression fractures, *J Spinal Disord* **17** (2004), 236–242.
[37] E. Waldorff, S. Goldstein and B. McCreadie, Age-dependent microdamage removal following mechanically induced microdamage in trabecular bone in vivo, *Bone* **40** (2007), 425–432.